*Journal of Statistical Physics, Vol. 113, Nos. 3/4, November 2003 (© 2003)*

# High Temperature Expansion for a Driven Bilayer System

**I. Mazilu**[1] **and B. Schmittmann**[2]

*Received January 22, 2003; accepted May 8, 2003*

Based directly on the microscopic lattice dynamics, a simple high temperature expansion can be devised for non-equilibrium steady states. We apply this technique to investigate the disordered phase and the phase diagram for a driven bilayer lattice gas at half filling. Our approximation captures the phases first observed in simulations, provides estimates for the transition lines, and allows us to compute signature observables of non-equilibrium dynamics, namely, particle and energy currents. Its focus on non-universal quantities offers a useful analytic complement to field-theoretic approaches.

**KEY WORDS:** Non-equilibrium steady states; driven lattice gases; high temperature series expansion.

## 1. INTRODUCTION

Many-particle systems in a state of thermal equilibrium are the exception, rather than the rule. Physical reality is overwhelmingly in a far-from-equilibrium state. Examples range from living cells and weather patterns to ripples on water and sand. As we leave the framework of standard Gibbs ensemble theory for equilibrium systems, we have to search for new avenues and tools, seeking to understand and classify non-equilibrium behavior. As a first step along this road, the study of the simplest generalizations of equilibrium systems, i.e., *non-equilibrium steady states* (NESS), has been particularly fruitful.[1,2] Progress has relied predominantly on simulations, mean-field theory and renormalization group analyses for simple model systems. A class of models which exhibit especially interesting

[1] Department of Physics and Engineering, Washington and Lee University, Lexington, Virginia 24450.

[2] Center for Stochastic Processes in Science and Engineering, Physics Department, Virginia Tech, Blacksburg, Virginia 24061-0435; e-mail: schmittm@vt.edu



0022-4715/03/1100-0505/0 © 2003 Plenum Publishing Corporation

behavior are driven diffusive systems. Microscopically, these are lattice gases, consisting of one or more species of particles and holes, whose densities are conserved. An external driving force, combined with suitable boundary conditions, maintains a NESS. In the simplest case,[3] a uniform bias, or drive, $E$, is imposed on an Ising lattice gas such that a nonzero steady-state mass current is induced. This model differs significantly from the usual Ising model: it displays generic long-range correlations,[3–5] and belongs to a non-equilibrium universality class[6] with upper critical dimension $d_c = 5$. The ordered phase is phase-separated into two strips of high vs. low density aligned with the bias. In contrast to equilibrium, bulk and interfacial properties are inextricably intertwined here.[7]

To avoid the complications due to the presence of interfaces, a bilayer structure was suggested:[8] in the two-dimensional case, a second lattice was introduced, allowing for particle-hole exchanges between each site and its mirror image. This bilayer system is half filled with particles, and both layers are driven in the same direction. In the absence of any energetic couplings between the two layers, it was hoped that typical ordered configurations would show *homogeneous* densities on each layer, one almost full and the other nearly empty. Remarkably, however, this expectation proved too naive: Monte Carlo simulations[9] showed a sequence of *two* phase transitions, as the temperature is lowered: the first transition takes the system from a disordered (D) phase to a strip-like (S) structure showing phase-separation *within each layer*, with interfaces parallel to the drive and "on top of" one another. The anticipated "full-empty" (FE) phase, with uniform densities on both layers, only emerges after a second transition which occurs at a lower temperature. Once an interaction $J$, of either sign, between nearest neighbors on different layers is introduced, the full phase diagram in $(J, E)$ space can be mapped out,[10, 11] using Monte Carlo simulations. As one might expect, the S (FE) phase dominates for attractive (repulsive) cross-layer coupling $J$. Remarkably, however, there is a small but finite region where the S-phase prevails even though the cross-layer coupling is weakly repulsive (cf. Fig. 1). The presence of this domain puts the two transitions, observed for $J = 0$, into perspective. We note for completeness that universal properties along the lines of continuous transitions have been analyzed in ref. 12 with the help of renormalized field theory.

To provide additional motivation for the study of layered structures, we note that multilayer models have a long history in equilibrium statistical mechanics.[13–15] On the theoretical side, they allow for the study of dimensional crossover;[16] on the more applied side, they provide natural models for the analysis of intercalated systems,[17] interacting solid surfaces or thin films.[18] Since intercalated systems are often driven by chemical gradients

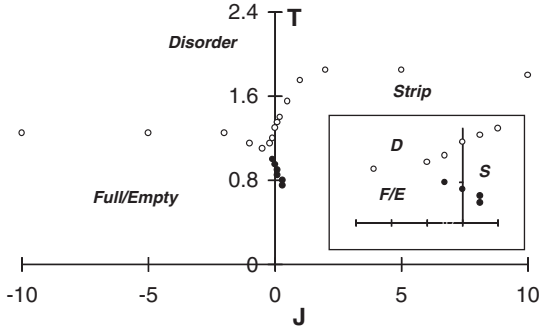


Fig. 1. The phase diagram of the driven bilayer lattice gas from Monte Carlo simulations,[10] at $J_0 = 1$ and infinite $E$. $T$ is measured in units of the Onsager temperature, $T_c(0)$. The domains of the three phases are indicated. The inset magnifies the vicinity of $J = 0$, $T = 1.0$ to demonstrate the shift of the bicritical point to negative $J$. Open (filled) circles indicate continuous (first order) transitions.

or electric fields, to speed the diffusion of foreign atoms into the host material, it is quite natural to study driven layered structures.

Simulations relie, of course, on discrete lattice models. In contrast, field theories operate in the continuum, and thus, all discrete degrees of freedom have to be coarse-grained before these powerful techniques can be applied. In the process, non-universal information is lost, such as, e.g., the location of transition lines in the phase diagram. It is therefore desirable to identify a second analytic approach which is based directly on the microscopic model and thus complements both simulations and continuum theories. Fortunately, high temperature expansion techniques[19] can be generalized to interacting driven lattice gases.[4, 20, 21] For the single-layer case, two-point correlation functions can be computed approximately[4, 20] and display the expected power law decays in the steady state. With some care, the approximate location of order-disorder transitions can be extracted and compared to simulation results.[20] Given the nature of the approximation, *quantitative* accuracy cannot be expected, but the *qualitative* agreement of data and approximation is remarkably good.

While the high temperature expansion is quite successful for the usual driven lattice gas, it is not clear to what extent it is capable of capturing the main features of other driven systems. This motivates the work presented in this paper, namely, the analysis of the bilayer system with this technique. Within a first-order approximation, we compute the two-point correlation functions and several related quantities, such as the particle current and the energy flux through the system. We extract the approximate location of the

continuous transition lines and compare our results to the Monte Carlo data. As in the single-layer case, the qualitative features of the transition lines are reproduced as well as can be expected. Some limitations of the method will be discussed.

This paper is organized as follows. We first introduce the bilayer model. After a brief summary of the high temperature expansion, we derive the closed set of equations satisfied by the two-point functions. We then obtain the solutions and extract the transition lines. Next, we show how the mass and energy currents through the system can be expressed in terms of pair correlations. We conclude with some comments and open questions.

## 2. THE BILAYER MODEL

A variant of the driven Ising model,[3] the model consists of two square lattices, one stacked above the other, resulting in a bilayer structure of size $L^2 \times 2$. Each lattice site $\vec{r} \equiv (x, y, z)$, with $x, y = 1, 2, \ldots, L$ and $z = 0, 1$, carries a spin variable $s(\vec{r}) = \pm 1$. Often, we also use lattice gas language, mapping spins into particles or holes. The total magnetization, $\sum_{\vec{r}} s(\vec{r})$, is fixed at zero so that the Ising critical point can be accessed. Within each layer, nearest-neighbor spins interact through a ferromagnetic exchange coupling $J_0 > 0$; in contrast, the cross-layer interaction $J$, which couples spins $s(x, y, 0)$ and $s(x, y, 1)$, can take both signs. These choices are motivated by the physics of intercalated systems.[17] Thus, the Hamiltonian of the system can be written in the form

$$H = -J_0 \sum_z \sum_{nn} s(x, y, z)\, s(x', y', z) - 2J \sum_{x, y} s(x, y, 0)\, s(x, y, 1) \qquad (1)$$

where $\sum_{nn}$ denotes the sum over all nearest-neighbor pairs $(x, y, z)$ and $(x', y', z)$ within the same plane. A heat bath at temperature $T$ is coupled to the system, in order to model thermal fluctuations. We use fully periodic boundary conditions in all directions; hence the factor of 2 in front of the cross-layer coupling $J$.

In the absence of the drive, particles hop to empty nearest-neighbor sites according to the usual Metropolis[22] rates, $\min\{1, \exp(-\beta\, \Delta H)\}$, where $\Delta H$ is the energy difference due to the jump. Respecting the conservation of density, the phase diagram of this system is easily found. At high temperatures, a disordered phase persists, characterized by correlations which fall off exponentially. At a critical temperature $T_c(J)$, a continuous transition occurs into the S (FE) phase for $J > 0$ ($J < 0$). At $J = 0$, the critical temperature takes the Onsager value[23] $T_c(0) = 2.269\ldots J_0/k_B$. For finite $J$, $T_c(J)$ is even in $J$, due to a simple gauge symmetry, and increases

monotonically with $|J|$. For $J \to \pm\infty$, nearest-neighbor spin pairs, with the partners located on different layers, combine into dimers who couple to neighboring dimers with strength $2J_0$. As a result, the critical temperature approaches the limit $T_c(\pm\infty) = 2T_c(0)$. The line $J = 0$, $T < T_c(0)$ is a line of first-order transitions between the S and FE phases. It ends in a bicritical point at $J = 0$, $T = T_c(0)$.

To drive the system out of equilibrium, we apply a bias (an "electric" field) $\vec{E}$ along the positive $x$-axis. The contents of two sites, $\vec{r}$ and $\vec{r}+\hat{a}$, separated by a (unit) lattice vector $\hat{a}$, are exchanged according to the rate

$$c(\vec{r}, \vec{r}+\hat{a}; \{s\}) = \min\{1, \exp[-\beta\, \Delta H + \tfrac{1}{2}\beta\hat{a}\cdot\vec{E}(s(\vec{r}) - s(\vec{r}+\hat{a}))]\} \qquad (2)$$

The argument $\{s\}$ reminds us that the rate depends on a local neighborhood of the central pair. Due to $E$, particle hops against the drive become unfavorable. In conjunction with periodic boundary conditions in the $x$- and $y$-directions, the system settles into a non-equilibrium steady state with a net particle current.

The phase diagram, resulting from Monte Carlo simulations at $J_0 = 1$ and infinite $E$, is shown in Fig. 1. The same phases and transitions are found, but the bicritical point and its attached first order line are shifted to higher $T$ and into the $J < 0$ region. Thus, the S phase is observed to be stable in a finite window of negative interlayer coupling, so that two transitions must occur along the $J = 0$ axis. This discovery represents the most unexpected new characteristic of this driven diffusive system. We also note the decrease of the critical temperatures for very large $|J|$. In a recent paper,[11] this phase diagram was extended to include *unequal intra-layer* attractive couplings. In this case, the bicritical point is shifted even further into the negative region of $J$ as the coupling transverse to the bias increases. In the following, we turn to an analysis in terms of a high temperature expansion.

## 3. HIGH TEMPERATURE EXPANSION

The dynamics underlying the Monte Carlo simulations is easily expressed via a master equation. The latter provides a convenient starting point for a high temperature expansion. For simplicity, we take the thermodynamic limit within each plane, i.e., $L \to \infty$. Following ref. 4, we first derive the equations of motion for the two-point functions. By virtue of the familiar hierarchy, they are coupled to the three-point functions; however, we will argue that these are negligible (while non-zero, they are numerically

rather small), so as to arrive at a closed system of equations for the two-point correlations. Temperature appears in these equations through the rates, via the combinations $\beta J$, $\beta J_0$, and $\beta E$. To preserve the non-equilibrium nature of our dynamics, we expand in $\beta J$ and $\beta J_0$, keeping $\beta E$ finite. Technically, this requires that $E$ always dominates the energetic contribution, i.e., $E > \Delta H$ for all jumps along $E$. To first order, a linear, *inhomogeneous* system of equations results, which can be solved exactly[20] and forms the basis of our analysis.

### 3.1. The Equations of Motion and Their Solution

Before turning to any detailed calculations, let us introduce the key quantities. The *two-point correlation function* is defined as:

$$G(\vec{r}-\vec{r}') = \langle s(\vec{r})\, s(\vec{r}')\rangle \tag{3}$$

where $\langle \cdot \rangle$ denotes the configurational average. $G$ is invariant under translations and under reflection of one or several lattice directions. At the origin, it is obviously unity, $G(\vec{0}) = \langle s^2(\vec{r})\rangle = 1$. We also introduce the Fourier transform of $G$, i.e., the *structure factor*:

$$S(k, p, q) \equiv \sum_{z=0,1} \sum_{x,\, y=-\infty}^{\infty} G(x, y, z)\, e^{-i(kx+py+qz)} \tag{4}$$

In the thermodynamic limit $L \to \infty$, the wave vectors $k$ and $p$ are continuous, but restricted to the first Brillouin zone $[-\pi, \pi]$, while $q$ is discrete, taking only the two values 0 and $\pi$. We also give the inverse transform,

$$\begin{aligned} G(x, y, z) &= \frac{1}{2(2\pi)^2} \sum_{q=0,\pi} \int_{-\pi}^{+\pi} dk \int_{-\pi}^{+\pi} dp\, S(k, p, q)\, e^{i(kx+py+qz)} \\ &\equiv \int S(k, p, q)\, e^{i(kx+py+qz)} \end{aligned} \tag{5}$$

where the second line just defines some simplified notation.

To set up the high temperature expansion, we first define the actual expansion parameters of our theory, namely

$$\begin{aligned} K_0 &\equiv \beta J_0 \\ K &\equiv \beta J \end{aligned} \tag{6}$$

For $K = K_0 = 0$, the steady state is known to be uniform for all $E$,[24] so that we are expanding about a well-defined zeroth order solution. The correlation functions and structure factors for this limit are trivial, namely, $G(\vec{r}) = \delta_{\vec{r},\vec{0}}$ where $\delta$ denotes the Kronecker symbol, and $S(k, p, q) = 1$. Hence $G(\vec{r})$ with $\vec{r} \neq \vec{0}$ is already of first order in the small parameter in the interacting case. Similarly, we can extract the zeroth order contribution from the structure factor, writing

$$S(k, p, q) = 1 + \tilde{S}(k, p, q) \tag{7}$$

so that $\tilde{S}$ carries the information about the interactions.

The exact equations of motion for $G$ are easily derived from the master equation:[4]

$$\frac{d}{dt}\langle s(\vec{r})\, s(\vec{r}')\rangle = \sum_{\vec{x},\vec{x}'} \langle s(\vec{r})\, s(\vec{r}')[s(\vec{x})\, s(\vec{x}') - 1]\, c(\vec{x}, \vec{x}'; \{s\})\rangle \tag{8}$$

Here, the sum runs over *nearest-neighbor* pairs $(\vec{x}, \vec{x}')$ such that $\vec{x} \in \{\vec{r}, \vec{r}'\}$ but $\vec{x}' \notin \{\vec{r}, \vec{r}'\}$. Stationary correlations are obtained by setting the left hand side to zero. Clearly, jumps along and against all three lattice directions will contribute to the right hand side of Eq. (8).

To proceed, let us write the jump rates in a form which makes their dependence on the spin configuration $\{s\}$ explicit, so that the configurational averages in Eq. (8) can be performed. For *finite* drive, our restriction $E > \Delta H$ ensures that jumps along $E$ occur with unit rate, while those against $E$ are suppressed by a factor of $\exp[-\beta(\Delta H + E)]$. Defining

$$\varepsilon \equiv e^{-\beta E} \tag{9}$$

the transition rates *parallel to the field* can be written as

$$c_{\parallel}(\vec{r}, \vec{r} + \hat{x}; \{s\}) = \frac{1}{4}[s(\vec{r}) - s(\vec{r} + \hat{x}) + 2] + \frac{\varepsilon}{4}[s(\vec{r} + \hat{x}) - s(\vec{r}) + 2] \exp(-\beta\, \Delta H) \tag{10}$$

where $\hat{x}$ is a unit vector in the positive $x$-direction. Transverse to the field we have two jump rates, corresponding to the directions $y$ and $z$. Both of these are regulated by the energy difference due to a jump:

$$c_{\perp}(\vec{r}, \vec{r} + \hat{a}; \{s\}) = \min\{1, \exp(-\beta\, \Delta H)\} \tag{11}$$

We are now ready to expand the rates in powers of $K$ and $K_0$ while keeping $\varepsilon$ finite:

$$c_{\|}(\vec{r}, \vec{r}+\hat{x}; \{s\}) = \frac{1}{4}[s(\vec{r}) - s(\vec{r}+\hat{x}) + 2]$$

$$+\frac{\varepsilon}{4}[s(\vec{r}+\hat{x}) - s(\vec{r}) + 2](1 - \beta\, \Delta H) + O(\beta^2) \qquad (12)$$

$$c_{\perp}(\vec{r}, \vec{r}+\hat{a}; \{s\}) = 1 - \frac{1}{2}\beta(\Delta H + |\Delta H|) + O(\beta^2) \qquad (13)$$

Given these simple forms for the rates, we can derive the equations of motion satisfied by the pair correlations directly from Eq. (8), following ref. 4. Keeping only corrections to first order in $K$, $K_0$ and neglecting three-point correlations, we obtain a *closed set of linear equations* for $G(x, y, z)$. Since the dynamics is restricted to nearest-neighbor processes, it is not surprising that the equations involve an anisotropic lattice Laplacian acting on $G(x, y, z)$. For $x, y, z$ near the origin, the Laplacian may include the origin and will thus generate inhomogeneities in the system of equations. The detailed form depends on the boundary conditions in $z$, and, of course, on the three parameters $K$, $K_0$, and $\varepsilon$. Below, we show the set of equations for fully periodic boundary conditions. The first three equations result from nearest neighbors of the origin, $\vec{r} = (1, 0, 0)$, $(0, 1, 0)$, and $(0, 0, 1)$:

$$\begin{aligned}
\partial_t G(1,0,0) &= (1+\varepsilon)[G(2,0,0) - G(1,0,0)] + 4[G(1,1,0) - G(1,0,0)] \\
&\quad + 4[G(1,0,1) - G(1,0,0)] + 2\varepsilon K_0 + 8K_0 \\
\partial_t G(0,1,0) &= 2(1+\varepsilon)[G(1,1,0) - G(0,1,0)] + 2[G(0,2,0) - G(0,1,0)] \\
&\quad + 4[G(0,1,1) - G(0,1,0)] + 4\varepsilon K_0 + 6K_0 \\
\partial_t G(0,0,1) &= 2(1+\varepsilon)[G(1,0,1) - G(0,0,1)] + 4[G(0,1,1) - G(0,0,1)] \\
&\quad + 8K + 8\varepsilon K
\end{aligned} \qquad (14)$$

By virtue of invariance under reflections, these equations also hold for the other nearest neighbors $\vec{r} = (-1, 0, 0)$, $(0, -1, 0)$, and $(0, 0, -1)$. The following three equations arise from the next-nearest neighbor sites, $\vec{r} = (1, 1, 0)$, $(0, 1, 1)$, and $(1, 0, 1)$, and their reflections:

$$
\begin{aligned}
\partial_t G(1,1,0) &= (1+\varepsilon)[G(2,1,0)+G(0,1,0)-2G(1,1,0)] \\
&\quad +2[G(1,2,0)+G(1,0,0)-2G(1,1,0)] \\
&\quad +4[G(1,1,1)-G(1,1,0)]-2K_0-2\varepsilon K_0 \\
\partial_t G(0,1,1) &= 2(1+\varepsilon)[G(1,1,1)-G(0,1,1)] \\
&\quad +2[G(0,2,1)+G(0,0,1)-2G(0,1,1)] \\
&\quad +4[G(0,1,0)-G(0,1,1)]-4[K_0+K] \\
\partial_t G(1,0,1) &= (1+\varepsilon)[G(2,0,1)+G(0,0,1)-2G(1,0,1)] \\
&\quad +4[G(1,1,1)-G(1,0,1)] \\
&\quad +4[G(1,0,0)-G(1,0,1)]-4\varepsilon K-4K_0
\end{aligned}
\tag{15}
$$

Increasing the separation of the participating sites further, to $\vec{r}=(2,0,0)$ and $(0,2,0)$, we obtain:

$$
\begin{aligned}
\partial_t G(2,0,0) &= (1+\varepsilon)[G(3,0,0)+G(1,0,0)-2G(2,0,0)] \\
&\quad +4[G(2,1,0)-G(2,0,0)]+4[G(2,0,1)-G(2,0,0)]-2\varepsilon K_0 \\
\partial_t G(0,2,0) &= 2(1+\varepsilon)[G(1,2,0)-G(0,2,0)] \\
&\quad +2[G(0,3,0)+G(0,1,0)-2G(0,2,0)] \\
&\quad +4[G(0,2,1)-G(0,2,0)]-2K_0
\end{aligned}
\tag{16}
$$

And finally, all $G$'s with $|x|+|y|+|z|>2$ satisfy homogeneous equations:

$$
\begin{aligned}
\partial_t G(i,j,k) &= (1+\varepsilon)[G(i+1,j,k)+G(i-1,j,k)-2G(i,j,k)] \\
&\quad +2[G(i,j+1,k)+G(i,j-1,k)-2G(i,j,k)] \\
&\quad +4[G(i,j,k-1)-G(i,j,k)]
\end{aligned}
\tag{17}
$$

The last equation contains the full anisotropic lattice Laplacian, acting on $G(i,j,k)$, without any inhomogeneities being generated. We note, for further reference, that the right hand sides of Eqs. (14)–(17) contain contributions from exchanges along and against the three lattice directions. Starting from Eq. (8), it is of course easy to keep track of terms originating in transverse vs. parallel jumps. Below, this distinction will become important when we turn to energy currents.

To solve this system, we closely follow the method presented in ref. 20. To summarize briefly, we express $G$ through its Fourier transform $\tilde{S}$ and

invoke the completeness of complex exponentials to project out an algebraic equation for $\tilde{S}(k, p, q)$. The three integrals

$$I_1 \equiv \int \tilde{S}(1-\cos k)$$

$$I_2 \equiv \int \tilde{S}(1-\cos p) \tag{18}$$

$$I_3 \equiv \int \tilde{S}(1-\cos q)$$

must be treated as unknowns for the time being. Defining the anisotropic lattice Laplacian in Fourier space,

$$\delta(k, p, q) \equiv 2(1+\varepsilon)(1-\cos k)+4(1-\cos p)+4(1-\cos q) \tag{19}$$

we can solve for $\tilde{S}$:

$$\tilde{S}(k, p, q) = \frac{L(k, p, q)}{\delta(k, p, q)} \tag{20}$$

where

$$\begin{aligned} L(k, p, q) \equiv\ & 2(1+\varepsilon)(1-\cos k)\, I_1 + 4(1-\cos p)\, I_2 + 4(1-\cos q)\, I_3 \\ & + (2\varepsilon K_0 + 8K_0)\, 2\cos k + (4\varepsilon K_0 + 6K_0)\, 2\cos p \\ & + (8\varepsilon K + 8K)\cos q - (2\varepsilon K_0 + 2K_0)\, 4\cos k \cos p \\ & - (4\varepsilon K + 4K_0)\, 2\cos k \cos q - 4(K_0 + K)\, 2\cos p \cos q \\ & - 4\varepsilon K_0 \cos 2k - 4K_0 \cos 2p \end{aligned} \tag{21}$$

Due to the appearance of the three integrals $I_1$, $I_2$, and $I_3$ in $L$, Eq. (20) is not yet a fully explicit solution for $\tilde{S}$. To determine these three coefficients, we need three linearly independent equations. One of these equations is given by the value of $G$ at the origin, $1 = G(0, 0, 0) = \int (1+\tilde{S})$, and the remaining two can be obtained directly from the definitions of $I_1$ and $I_3$ in Eq. (18):

$$\begin{aligned} 0 &= \int \frac{L(k, p, q)}{\delta(k, p, q)} \\ 0 &= -I_1 + \int \frac{L(k, p, q)}{\delta(k, p, q)} (1-\cos k) \\ 0 &= -I_3 + \int \frac{L(k, p, q)}{\delta(k, p, q)} (1-\cos q) \end{aligned} \tag{22}$$

After inserting Eq. (21) for $L$, this leads to a set of three inhomogeneous, linear equations for the three $I$'s, which are easily solved by a matrix inversion. Omitting some lengthy details, we just note the following overall features: (i) All three coefficients are functions of $K$, $K_0$, and $\varepsilon$; (ii) for the whole range of fields $\varepsilon$ and for $K_0 = 1$ and $K = \pm 1$ (attractive and repulsive inter-layer interactions), $I_1$ and $I_2$ are negative, while $I_3$ is positive for $K = -1$ and negative for $K = +1$.

This concludes the calculation of the structure factor. To summarize, we obtain

$$S(k, p, q) = 1 + \frac{L(k, p, q)}{\delta(k, p, q)} + O(K^2, K_0^2, KK_0) \tag{23}$$

Even at the lowest nontrivial order, this solution carries a significant amount of information about our system. For example, we note that the anisotropic momentum dependence of numerator and denominator leads to power law correlations in the $x$- and $y$-directions.[4, 20, 25] Focusing specifically on the phase diagram, we show in the following how to extract an approximate shape of the critical lines.

### 3.2. The Critical Lines

For the bilayer system, we need to identify, and distinguish, *two types* of continuous transitions, namely, from disorder (D) into the strip (S) and the full-empty (FE) phases, respectively. Since the D-S transition is marked by the appearance of phase-separated strips in each layer, aligned with the driving force, it can be located by seeking singularities in $\lim_{p \to 0} S(0, p, 0)$. In contrast, the D-FE transition exhibits homogeneous, but opposite magnetizations in the two planes, so that it can be found by considering $S(0, 0, \pi)$. Not surprisingly, these two structure factors are precisely the order parameters chosen in the MC studies.[10]

Yet, another subtlety must be considered: in a typical high temperature expansion such as ours, only a finite number of terms can be computed. Hence, any perturbative result for the structure factor must be finite, and instead, the radius of convergence of the expansion must be estimated. Even this is not practical here, since we have only two terms of the series. To circumvent these restrictions,[20] we extract the singularity by looking for *zeros* of $S^{-1}$, to first order in $K$ and $K_0$.

Starting from Eq. (23), we obtain

$$S^{-1}(k, p, q) = 1 - \frac{L(k, p, q)}{\delta(k, p, q)} + O(K^2, K_0^2, KK_0) \tag{24}$$

and seek to locate the zeros of $\lim_{p\to 0} S^{-1}(0, p, 0)$ for the D-S transition, and of $S^{-1}(0, 0, \pi)$ for the D-FE transition. Of course, we should ensure that these are the first zeros which are encountered upon lowering the temperature. Therefore, we consider, more generally, the behavior of $S^{-1}(k, p, q)$ at small $k$, $p$ and fixed $q$. Since the zeros of $S^{-1}$ are obviously identical to those of $\delta - L$ in Eq. (24), we compute the appropriate limits from Eqs. (19) and (21). Introducing some simplified notation, we write

$$\lim_{k,p\to 0} [\delta(k, p, q) - L(k, p, q)] \equiv \tau_{\|}(q)\, k^2 + 2\tau_{\perp}(q)\, p^2 + 4\tau_z(1-\cos q) + O(k^4, p^4, k^2p^2) \tag{25}$$

and read off

$$\begin{aligned} \tau_{\|}(q) &= (1+\varepsilon)(1-I_1) - 10\varepsilon K_0 + 4K_0 - (4\varepsilon K + 4K_0)\cos q \\ \tau_{\perp}(q) &= 1 - I_2 - 3K_0 - (2K_0 + 2K)\cos q \\ \tau_z &= 1 - I_3 - 4K_0 \end{aligned} \tag{26}$$

In a field-theoretic context,[12] these quantities play the role of diffusion coefficients: $\tau_{\|}$ and $\tau_{\perp}$ control the in-plane diffusion in the parallel and transverse directions, respectively, while $\tau_z$ controls the cross-plane hopping.

For high temperatures, i.e., small values of $K_0 = \beta J_0$ and $K = \beta J$, all three $\tau$-coefficients are positive. Seeking zeros of these expressions, as $K_0$ and $K$ increase, we need to consider the two cases $q = 0$ and $q = \pi$ separately. For $q = 0$, we find that $\tau_{\perp}(0)$ has a single zero at a critical $\beta_c^{\mathrm{S}}$, for given $J_0$, $J$, and $\varepsilon$. At these parameter values, $\tau_{\|}(0)$ and $\tau_z$ remain positive. Similarly, for $q = \pi$, the coefficient $\tau_z$ is the one which vanishes first as $\beta$ increases, reaching zero at a critical $\beta_c^{\mathrm{FE}}$. Converting into temperatures, we obtain two functions, $T_c^{\mathrm{S}}(J_0, J, \varepsilon)$ and $T_c^{\mathrm{FE}}(J_0, J, \varepsilon)$, and we need to identify the larger of the two: If $\max[T_c^{\mathrm{S}}(J_0, J, \varepsilon), T_c^{\mathrm{FE}}(J_0, J, \varepsilon)] = T_c^{\mathrm{S}}(J_0, J, \varepsilon)$, the order-disorder transition is of the D-S type. Otherwise, if $\max[T_c^{\mathrm{S}}(J_0, J, \varepsilon), T_c^{\mathrm{FE}}(J_0, J, \varepsilon)] = T_c^{\mathrm{FE}}(J_0, J, \varepsilon)$, the FE phase is selected upon crossing criticality.

While the two critical lines, $T_c^{\mathrm{S}}(J_0, J, \varepsilon)$ and $T_c^{\mathrm{FE}}(J_0, J, \varepsilon)$, can in principle be found analytically, the details are not particularly illuminating. Instead, we present a range of numerical results below. For example, for infinite $E$ ($\varepsilon = 0$), we obtain

$$\begin{aligned} k_B T_c^{\mathrm{S}}(J_0, J, 0) &= 4.39 J_0 + 2.11 J \\ k_B T_c^{\mathrm{FE}}(J_0, J, 0) &= 4.14 J_0 - 1.36 J \end{aligned} \tag{27}$$

For finite $E$ with $\varepsilon = \exp(-\beta E) = 0.5$, all coefficients decrease and we find

$$\begin{aligned} k_B T_c^{\mathrm{S}}(J_0, J, 0.5) &= 4.15 J_0 + 2.03 J \\ k_B T_c^{\mathrm{FE}}(J_0, J, 0.5) &= 4.05 J_0 - 1.70 J \end{aligned} \tag{28}$$

In each case, the bicritical point is defined through the solution of $T_c^{\mathrm{S}}(J_0, J, \varepsilon) = T_c^{\mathrm{FE}}(J_0, J, \varepsilon)$. For comparison, we also quote the equilibrium ($E = 0$) results:

$$\begin{aligned} k_B T_c^{\mathrm{S}}(J_0, J, 1) &= 4 J_0 + 2 J \\ k_B T_c^{\mathrm{FE}}(J_0, J, 1) &= 4 J_0 - 2 J \end{aligned} \tag{29}$$

which exhibit the expected $J \to -J$ symmetry.

Recalling that the MC simulations were performed at fixed, positive in-plane coupling $J_0$, we need to consider only the dependence on the cross-plane coupling $J$ which may take either sign. All of our results show that, for positive $J$, the D-S transition dominates while, for *sufficiently negative* $J$, a D-FE transition is found. In the following, we discuss the non-equilibrium ($E \neq 0$) results in more detail.

Figure 2 shows the critical lines for two typical values of the parameters, $\varepsilon = 0.5$ and $J_0 = 1$. Being the result of a first order approximation, the critical lines must of course be linear in $J$. Therefore, quantitative agreement with the simulation data cannot be expected; nevertheless, several important features are reproduced: *the existence of two ordered phases* and the *shift of the bicritical point* to higher values of $T$ and negative $J$. As a result, the S phase survives for small, negative $J$, despite being energetically unfavorable. This phenomenon can be explained qualitatively[10] by noting that *long-range negative* correlations transverse to $E$ dominate the ordering process for positive $J$, and this mechanism continues to be effective for a small region of negative $J$. For large and negative $J$, the disordered state orders into the full-empty (FE) phase, characterized by the planes being mainly full or empty. Finally, we comment on the dependence of the critical lines, specifically $T_c^{\mathrm{S}}(1, 1, \varepsilon)$ and $T_c^{\mathrm{FE}}(1, -1, \varepsilon)$, on the field parameter $\varepsilon = \exp(-\beta E)$, shown in Fig. 3. For $E = 0$, both temperatures are equal, by virtue of the $J \to -J$ symmetry of the equilibrium system. As the field becomes stronger, the critical temperature of the D-S transition increases, in contrast to the critical temperature of the D-FE transition which decreases. This behavior agrees qualitatively with the trend observed in the simulations.[10, 26]

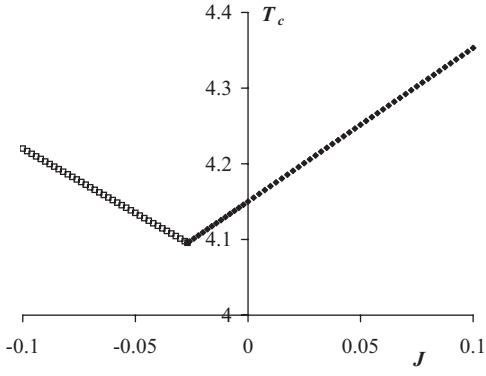


Fig. 2. The dependence of the critical temperature, $\max[T_c^{\mathrm{S}}(J_0, J, \varepsilon), T_c^{\mathrm{FE}}(J_0, J, \varepsilon)]$, on the cross-layer coupling $J$, for $\varepsilon = 0.5$ and $J_0 = 1$. Filled diamonds (open squares) indicate that the transition is of the D-S (D-FE) type. Critical temperatures for $J > 0.1$ ($J < -0.1$) can be obtained by linear extrapolation of the D-S (D-FE) branch.

There are several other quantities of physical interest which are immediately related to the two-point correlations, such as the steady-state particle and energy currents. To extract these, we first discuss the inverse Fourier transform of the structure factor, focusing specifically on the nearest-neighbor correlations.

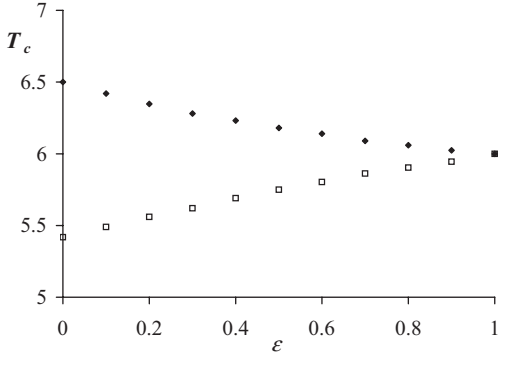


Fig. 3. The critical temperatures, $T_c^{\mathrm{S}}(1, 1, \varepsilon)$ corresponding to a D-S transition (filled diamonds) and $T_c^{\mathrm{FE}}(1, -1, \varepsilon)$ corresponding to a D-FE transition (open squares) as functions of the field parameter $\varepsilon = \exp(-\beta E)$.

### 3.3. Related Physical Observables

*Nearest-Neighbor Correlations.* These are easily found from our solution for the structure factor, Eq. (23). For example, the nearest-neighbor correlation in the field direction is given by:

$$G(1, 0, 0) = \int \tilde{S}(k, p, q) \cos k + O(K^2, K_0^2, KK_0) \tag{30}$$

Since $\int \tilde{S} = 0$ by virtue of $G(0, 0, 0) = 1$, we obtain $G(1, 0, 0) = -I_1$ and similarly, $G(0, 1, 0) = -I_2$ and $G(0, 0, 1) = -I_3$, all to first order. These three integrals are already known since they were required for the discussion of the critical lines. Specifically, for $\varepsilon = 0.5$ we find, neglecting corrections of $O(K^2, K_0^2, KK_0)$:

$$\begin{aligned} G(1, 0, 0) &= 0.949K_0 + 0.030K \\ G(0, 1, 0) &= 0.849K_0 - 0.034K \\ G(0, 0, 1) &= -0.055K_0 + 1.702K \end{aligned} \tag{31}$$

For reference, we also quote the first order results for the equilibrium ($E = 0$) correlations:

$$\begin{aligned} G^{eq}(1, 0, 0) &= G^{eq}(0, 1, 0) = K_0 \\ G^{eq}(0, 0, 1) &= 2K \end{aligned} \tag{32}$$

Figure 4 shows the drive dependence of the three *nearest-neighbor* correlation functions, at $K_0 = 1$ and $K = \pm 1$, to illustrate their behavior in two typical domains (attractive and repulsive cross-layer coupling). Of course, these values of $K$ and $K_0$ are not "small," but in a linear approximation they just serve to fix a scale. Consistent with the interpretation of the drive as an additional noise which tends to break bonds, all correlations are reduced compared to their equilibrium value. Further, as the field is switched on, the $J \to -J$ symmetry of the equilibrium system is broken, and the correlations for repulsive and attractive cross-layer coupling differ from one another. The details of how they differ provides some insight into the ordered phases which will eventually emerge.

The first plot (Fig. 4a) shows the correlation function for a nearest-neighbor bond within a given plane, aligned with the drive direction. It is interesting to note that the correlations for repulsive cross-layer coupling are more strongly suppressed than their counterparts for attractive $J$. This feature becomes more transparent when we consider nearest-neighbor correlations transverse to the drive, but still within the same plane (Fig. 4b).

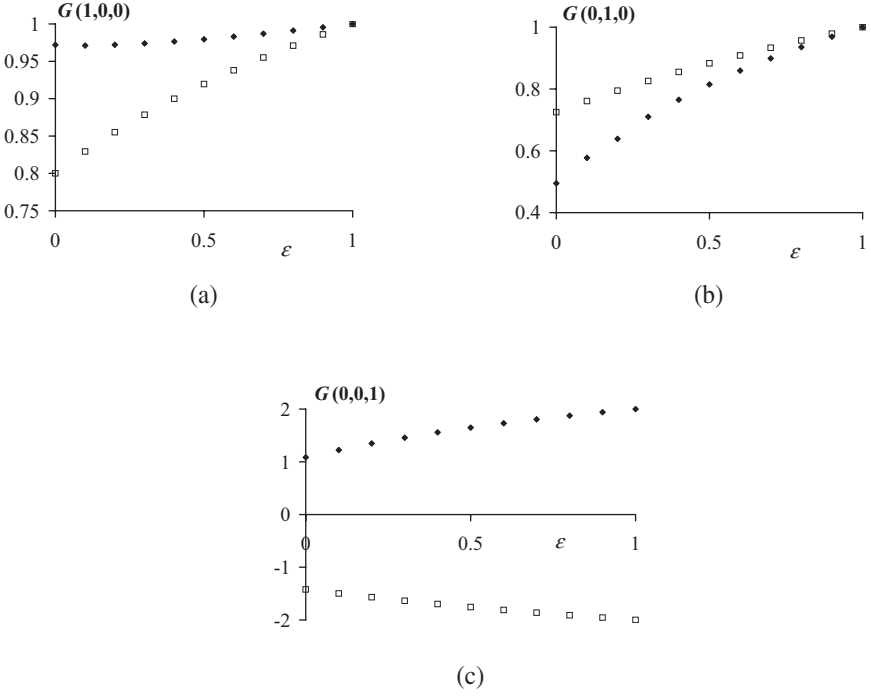


Fig. 4. Nearest-neighbor pair correlations along the (a) $x$-, (b) $y$-, and (c) $z$-axes, as functions of the drive parameter $\varepsilon$, for $K_0 = |K| = 1$. Filled diamonds (open squares) refer to ferromagnetic (antiferromagnetic) cross-layer coupling $K = +1$ ($K = -1$).

For attractive cross-layer coupling, we note that $G(1, 0, 0)$ is considerably enhanced over $G(0, 1, 0)$, while the two correlations are roughly equal in the repulsive case. This indicates a tendency to form droplets of correlated spins which are elongated in the field direction for $J = +1$ while remaining approximately isotropic for $J = -1$, hinting at the nature of the associated ordered phases (strip-like vs. uniform within each layer). This picture is completed when we consider the cross-plane correlations $G(0, 0, 1)$ (Fig. 4c): These are positive in the attractive, and negative in the repulsive case, demonstrating the tendency towards equal vs. opposite local magnetizations on the two layers. Given that we have performed only a first order calculation, the results really carry a remarkable amount of information about the system. Encouraged by these observations, we now consider two other quantities, namely, the particle and energy currents.

*The Particle Current.* Due to the bias in conjunction with periodic boundary conditions, the bilayer system carries a net particle current, $\langle j \rangle$.

Since only nearest-neighbor exchanges are possible, this current is proportional to the density (number per site) of available particle-hole pairs in the field direction. The transition rate $c_{\|}$ along this direction, given in Eq. (10), then counts the fraction of these pairs which will actually exchange per unit time. Specifically, in configuration $\{s\}$, the particle current can be written as

$$j(\{s\}) = \frac{1}{2L^2} \sum_{\vec{r}} \frac{s(\vec{r}) - s(\vec{r}+\hat{x})}{2} c_{\|}(\vec{r}, \vec{r}+\hat{x}; \{s\}) \tag{33}$$

For infinite $E$, this expression simplifies considerably, since jumps against the field will be completely suppressed.

After a few straightforward algebraic manipulations, the *average current* can be expressed through the pair correlations along the field direction. To *first order* in $K$ and $K_0$, we obtain

$$\langle j \rangle = \tfrac{1}{4}(1-\varepsilon)[1 - G(1, 0, 0)] + O(K^2, K_0^2, K_0 K) \tag{34}$$

which shows that it is non-zero only if $E \neq 0$. Further, it takes its maximum value at infinite temperature and is reduced by (attractive) nearest-neighbor interactions. The graph (Fig. 5) shows the field-dependence of this current, for $K_0 = 1$ and $K = \pm 1$. Since nearest-neighbor correlations along the field are much larger for positive $J$, indicating a predominance of particle-particle or hole-hole pairs, the current is reduced relative to the repulsive case.

*Energy Currents.* Another interesting quantity associated with driven dynamics is the change in configurational *energy* during one Monte Carlo

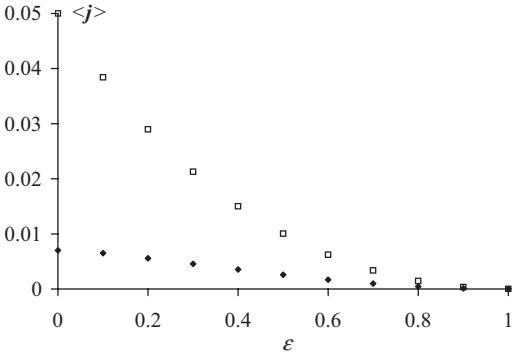


Fig. 5. The average particle current, $\langle j \rangle$, vs. the drive parameter $\varepsilon$, for $K_0 = |K| = 1$. Filled diamonds (open squares) refer to ferromagnetic (antiferromagnetic) cross-layer coupling.

step. In the steady state, by definition, the average configurational energy is of course constant. However, particle-hole exchanges *parallel* to the field direction tend to increase the energy, since the drive can easily break bonds. In contrast, exchanges *transverse* to $E$ are purely energetically driven and hence, prefer to satisfy bonds so that the energy decreases.[1] In summary, we have

$$\left\langle \frac{dH}{dt} \right\rangle_{\parallel} = -\left\langle \frac{dH}{dt} \right\rangle_{\perp} > 0 \tag{35}$$

Even if a particle current were absent, the presence of energy currents would signal the *non-equilibrium* steady state.

Since the configurational energy involves only nearest-neighbor bonds, it is obvious that only the time evolution of nearest-neighbor correlations plays a role in these two fluxes. Specifically, we have

$$L^{-2}\left\langle \frac{dH}{dt} \right\rangle_{\parallel} = -J_0 \left(\frac{\partial}{\partial t}\right)_{\parallel} [G(1,0,0)+G(0,1,0)] - 2J \left(\frac{\partial}{\partial t}\right)_{\parallel} G(0,0,1) \tag{36}$$

where the subscript on the time derivatives reminds us to select only those processes which are due to parallel exchanges alone. These can be easily identified from the terms contributing to Eq. (8) or (14). Of course, there is an analogous equation for $\langle dH/dt \rangle_{\perp}$. Collecting the relevant contributions and multiplying both sides by the inverse temperature $\beta$ to express everything in terms of $K_0$ and $K$, we find:

$$\begin{aligned} L^{-2}\left\langle \frac{d\beta\, H}{dt} \right\rangle_{\parallel} = & -K_0\{(1+\varepsilon)[G(2,0,0)-G(1,0,0)] \\ & +2(1+\varepsilon)[G(1,1,0)-G(0,1,0)]+6\varepsilon K_0\} \\ & -2K\{2(1+\varepsilon)[G(1,0,1)-G(0,0,1)]+8\varepsilon K\} \end{aligned} \tag{37}$$

The correlation functions spanning next- and next-next nearest neighbors which appear here can again be determined from our solution for the structure factors. The result, at $K_0 = 1$ and $K = \pm 1$, is shown in Fig. 6 as a function of $\varepsilon$. As expected, this flux is always non-negative and monotonically increasing as a function of $E$. We note that the current for $K = -1$ is slightly larger than its counterpart for $K = +1$. Since it is a complicated function of the couplings and several correlations, we cannot offer a simple intuitive explanation of this property.

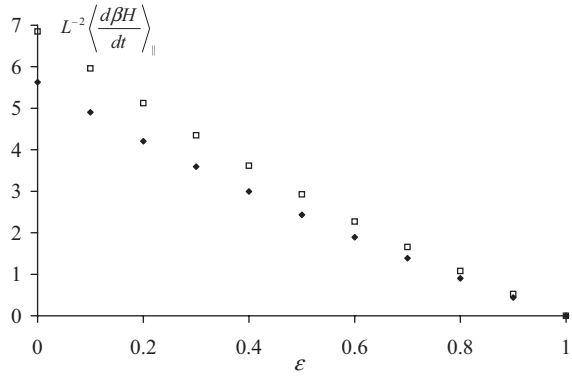


Fig. 6. The average energy current, $L^{-2}\langle d\beta\, H/dt\rangle_{\|}$, vs. the drive parameter $\varepsilon$, for $K_0 = |K| = 1$. Filled diamonds (open squares) refer to ferromagnetic (antiferromagnetic) cross-layer coupling.

## 4. CONCLUDING REMARKS

Based directly on the microscopic lattice dynamics, the high temperature series provides us with a simple analytic tool which complements field theoretic approaches. Even in a first order approximation, it is remarkable how many features of the MC results are—at least qualitatively—reproduced. To summarize our results briefly, we derive, and solve, a set of equations for the stationary pair correlation functions and their Fourier transforms, the equal-time structure factors. By matching the series expansion of the latter with the expected critical singularity, we find two critical lines, separating the disordered phase from the strip phase (S) and the full-empty phase (FE), respectively. We also observe the shift of the bicritical point which marks the juncture of these two lines, in very good qualitative agreement with the simulations. To illustrate the non-equilibrium character of the steady state, we compute the particle current and the energy flux through the system. The particle current is determined by the nearest-neighbor correlations in the field direction, and takes its maximum value in the absence of interactions. Our findings for the energy current confirm intuitive expectations: parallel exchanges tend to increase, while transverse exchanges tend to lower, the configurational energy.

A brief comment on boundary conditions is in order. Even though it is quite natural to use periodic boundary conditions in all lattice directions, it is not unreasonable to consider other choices, especially in the $z$-direction. To recall, periodicity in $z$ implies that the site $(x, y, 0)$ is connected to the site $(x, y, 1)$ via *two* bonds which enter into *both* the energetics *and* and the dynamics (i.e., there are two channels for a particle to move from one layer

to the other). Alternately, we can choose open boundary conditions in $z$ and consider only a single energetic bond and single dynamical channel between these two sites. Mixtures of these two cases can also be constructed: i.e., imposing periodic boundary conditions on the energetics, but allowing only a single channel for particle moves, or vice versa. The first (second) "mixed" case is reducible to the case of open (periodic) boundary conditions, with $J$ replaced by $2J$ $(J/2)$. Even though details are not presented here, we did, in fact, compute the critical lines for different cross-plane boundary conditions. The main conclusions of our study, namely, the existence of the two continuous phase transitions and the shift of the bicritical point, hold for all of these variations.

The high temperature expansion presented here has two shortcomings. First, our results provide no insight into the first-order transitions between the FE and S phases which were observed in the simulations. As in all high temperature series, the first singularity which is encountered as $T$ is lowered determines the radius of convergence. A low-temperature approach would be necessary to capture transitions between ordered phases. Second, our series is currently limited to just one nontrivial term. In order to compute the second order correction to the pair correlations, we would need to know the full stationary distribution, $P^*$, to first order. Writing the stationary master equation in the form $0 = LP^*$ where $L$ is the linear operator ("Liouvillean") defined by the transition rates, this requires the full inverse of $L$, to zeroth order. Finding this inverse is a highly nontrivial (and as yet unsolved) problem.

Inspite of these drawbacks, the high temperature expansion is one of the few analytic tools which provide insight into non-equilibrium steady states. It is conceptually and mathematically straightforward, and—at least at the qualitative level—surprisingly reliable. Since it is based directly on the microscopic lattice dynamics, it still carries information about nonuniversal properties which would be lost upon taking a continuum limit. It is therefore a valuable complement to both simulations and field theoretic methods.

## ACKNOWLEDGMENTS

We thank U. C. Täuber and R. K. P. Zia for fruitful discussions. Financial support from the NSF through the Division of Materials Research is gratefully acknowledged.

## REFERENCES

1. B. Schmittmann and R. K. P Zia, in *Phase Transitions and Critical Phenomena*, Vol. 17, C. Domb and J. L. Lebowitz, eds. (Academic Press, London, 1995).

2. D. Mukamel, in *Soft and Fragile Matter: Nonequilibrium Dynamics, Metastability and Flow*, M. E. Cates and M. R. Evans, eds. (Institute of Physics Publishing, Bristol, 2000); J. Marro and R. Dickman, *Nonequilibrium Phase Transitions in Lattice Models* (Cambridge University Press, Cambridge, 1999).
3. S. Katz, J. L. Lebowitz, and H. Spohn, *Phys. Rev. B* **28**:1655 (1983) and *J. Stat. Phys.* **34**:497 (1984).
4. M. Q. Zhang, J.-S. Wang, J. L. Lebowitz, and J. L. Vallès, *J. Stat. Phys.* **52**:1461 (1988).
5. P. L. Garrido, J. L. Lebowitz, C. Maes, and H. Spohn, *Phys. Rev. A* **42**:1954 (1990).
6. H.-K. Janssen and B. Schmittmann, *Z. Phys. B* **64**:503 (1986); K.-t. Leung and J. L. Cardy, *J. Stat. Phys.* **44**:567 (1986) and **45**:1087 (1986) (erratum).
7. J. L. Vallès, K.-t. Leung, and R. K. P. Zia, *J. Stat. Phys.* **56**:43 (1989).
8. K. K. Mon, private communication (1991).
9. A. Achahbar, P. L Garrido, and J. Marro, *Phys. Lett. A* **172**:29 (1992); A. Achahbar and J. Marro, *J. Stat. Phys.* **78**:1493 (1995).
10. C. C. Hill, R. K. P. Zia, and B. Schmittmann, *Phys. Rev. Lett.* **77**:514 (1996). See also B. Schmittmann, C. C. Hill, and R. K. P. Zia, *Physica A* **239**:382 (1997).
11. C.-P. Chng and J.-S. Wang, *Phys. Rev. E* **61**:4962 (2000).
12. U. C. Täuber, B. Schmittmann, and R. K. P. Zia, *J. Phys. A* **34**:L583 (2001).
13. L. E. Ballentine, *Physica* **30**:1231 (1964).
14. K. Binder, *Thin Solid Films* **20**:367 (1974).
15. P. L. Hansen, J. Lemmich, J. H. Ipsen, and O. G. Mouritsen, *J. Stat. Phys.* **73**:723 (1993). This article also gives a brief history and further references.
16. T. W. Capehart and M. E. Fisher, *Phys. Rev. B* **13**:5021 (1976).
17. M. S. Dresselhaus and G. Dresselhaus, *Adv. Phys.* **30**:139 (1981); G. R. Carlow and R. F. Frindt, *Phys. Rev. B* **50**:11107 (1994). See also G. R. Carlow, *Intercalation Channels in Staged Ag Intercalated $TiS_2$*, Ph.D. thesis (Simon Frasier University, 1992).
18. A. Ferrenberg and D. P. Landau, *J. Appl. Phys.* **70**:6215 (1991).
19. See, especially, C. Domb, D. S. Gaunt, and A. J. Guttmann, in *Phase Transitions and Critical Phenomena*, Vol. 3, C. Domb and M. S. Green, eds. (Academic, London, 1974); and A. J. Guttmann, in *Phase Transitions and Critical Phenomena*, Vol. 13, C. Domb and J. L. Lebowitz, eds. (Academic Press, London, 1989).
20. B. Schmittmann and R. K. P. Zia, *J. Stat. Phys.* **91**:525(1998).
21. L. B. Shaw, B. Schmittmann, and R. K. P. Zia, *J. Stat. Phys.* **95**:981 (1999).
22. N. Metropolis, A. W. Rosenbluth, M. M. Rosenbluth, A. H. Teller, and E. Teller, *J. Chem. Phys.* **21**:1097 (1953).
23. L. Onsager, *Phys. Rev.* **65**:117 (1944); B. M. McCoy and T. T. Wu, *The Two-Dimensional Ising Model* (Harvard University Press, Cambridge, MA, 1973).
24. F. Spitzer, *Adv. Math.* **5**:246 (1970).
25. J. J. Alonso, P. L. Garrido, J. Marro, and A. Achahbar, *J. Phys. A* **28**:4669 (1995).
26. C. C. Hill, *Phase Transitions in Driven Bi-Layer Systems* Honors Thesis (Virginia Tech, 1996).